



(72) Rubin, William L., US

(72) Leyh, Carl H., US

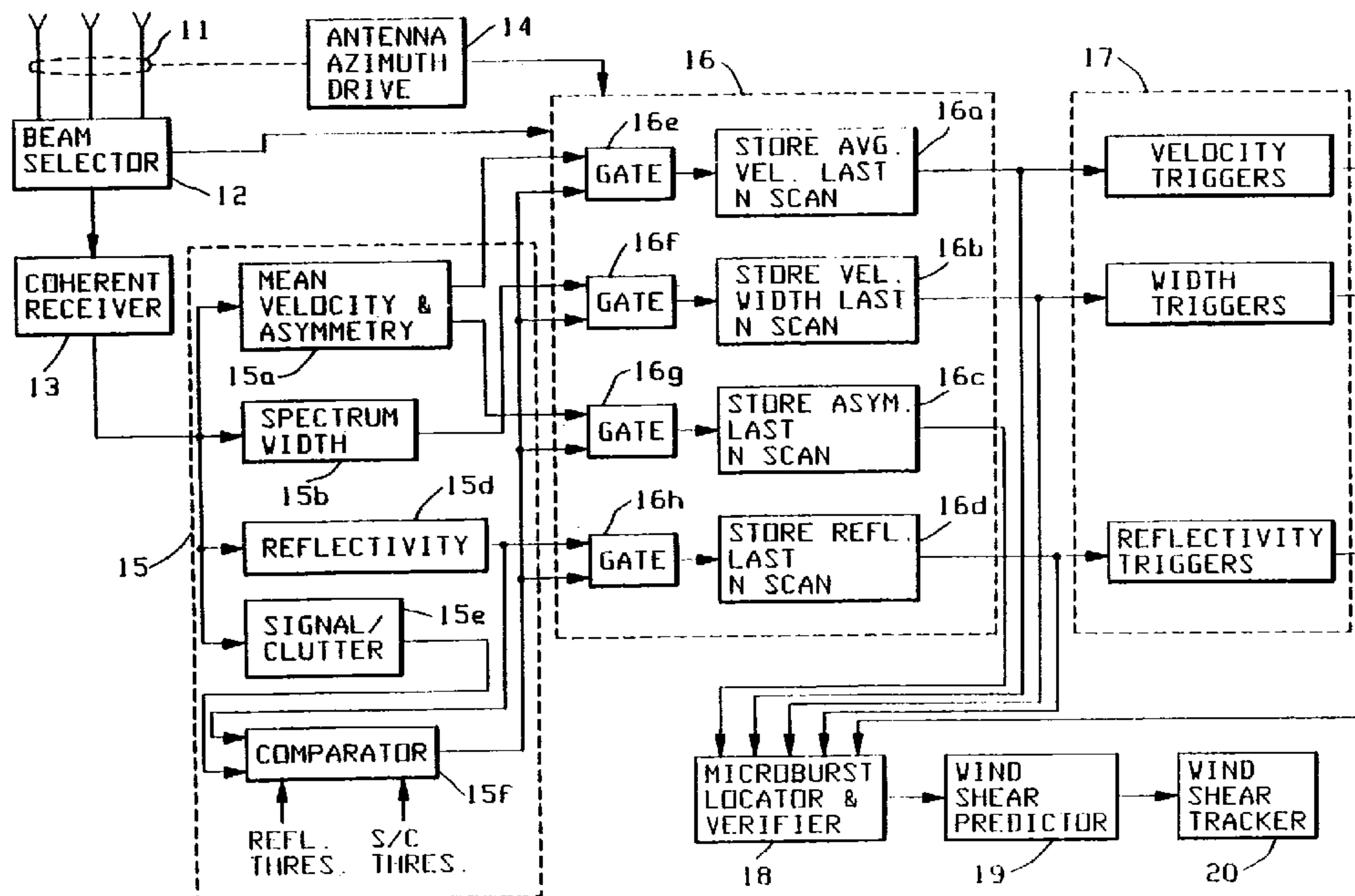
(73) Loral Corporation, US

(51) Int.Cl.<sup>5</sup> G01S 13/95

(30) 1991/04/09 (683,356) US

(54) **DETECTEUR DE PRECURSEURS EN MICROSALVES  
UTILISANT DES FAISCEAUX RADAR**

(54) **MICROBURST PRECURSOR DETECTOR UTILIZING  
MICROWAVE RADAR**



(57) Un détecteur de signes précurseurs de microrafales "microburst" utilise une multiplicité de faisceaux de radar (1-4), échantillonne dans chaque faisceau des informations de radar provenant de réflecteurs de signaux de radar météorologique, et traite (16) les signaux d'informations sur une base statistique afin de

(57) A microburst precursor detector utilizes a multiplicity of radar beams (1-4) and samples radar returns, in each beam, from meteorological radar signal reflectors and processes (16) the signal returns in a statistical manner to determine average radar reflectivity and to extract doppler signal parameters. These





(11) (21) (C) **2,107,586**  
(86) 1992/04/06  
(87) 1992/10/10  
(45) 2000/03/14

déterminer le pouvoir réfléchissant moyen du radar et d'extraire des paramètres de signaux Doppler. Ces paramètres sont utilisés pour déterminer un second ensemble de paramètres: la fréquence Doppler moyenne dans chaque faisceau de radar, l'étendue spectrale Doppler dans chaque faisceau de radar et l'obliquité du spectre Doppler dans chaque faisceau. Le second ensemble de paramètres est traité (18-20) afin d'établir l'existence d'une microrafale, l'impact prévu à la surface, le temps restant avant l'impact, l'emplacement et la trajectoire à la surface du cisaillement du vent et l'ampleur du cisaillement du vent.

parameters are utilized to determine a second set of parameters; average doppler frequency within each radar beam, doppler spectral spread within each radar beam, and the skewness of the doppler spectrum in each beam. The second set of parameters is processed (18-20) to establish the existence of a microburst, predicted surface impact, time to impact, wind shear surface location and track, and the magnitude of the wind shear.





INTERNATIONAL APPLICATION PUBLISHED UNDER THE PATENT COOPERATION TREATY (PCT)

(51) International Patent Classification <sup>5</sup> :  
G01S 13/95

A1

(11) International Publication Number: WO 92/18877  
(43) International Publication Date: 29 October 1992 (29.10.92)

(21) International Application Number: PCT/US92/02748

(22) International Filing Date: 6 April 1992 (06.04.92)

(30) Priority data:  
683,356 9 April 1991 (09.04.91) US

(71) Applicant: UNISYS CORPORATION [US/US]; Township Line and Union Meeting Roads, P.O. Box 500, Blue Bell, PA 19424 (US).

(72) Inventors: RUBIN, William, L. ; 166-47 16th Avenue, Whitestone, NY 11357 (US). LEYH, Carl, H. ; 89 Magnolia Avenue, Floral Park, NY 11001 (US).

(74) Agent: STARR, Mark, T.; Unisys Corporation, Township Line and Union Meeting Roads, P.O. Box 500, Blue Bell, PA 19424 (US).

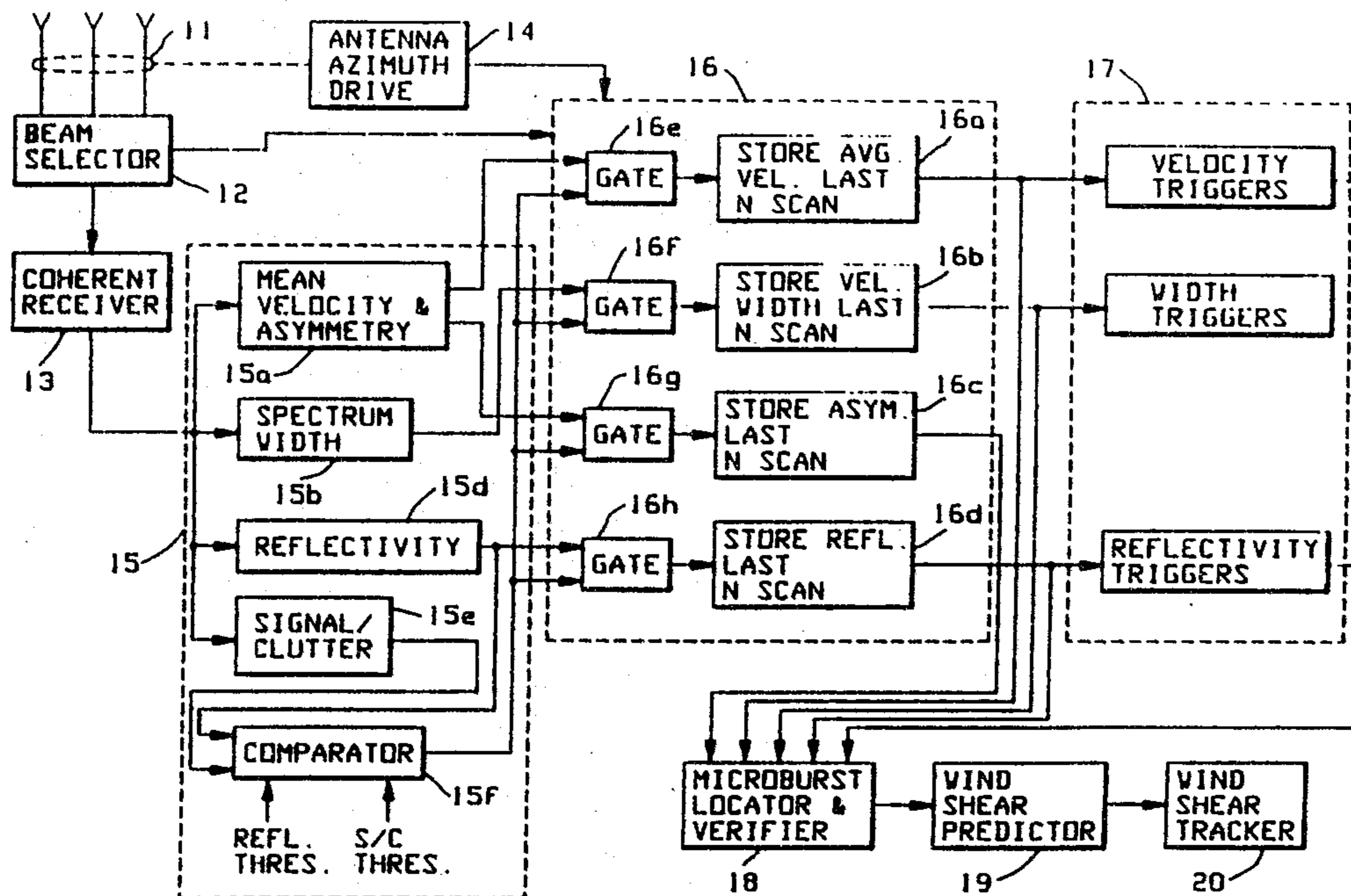
(81) Designated States: AT (European patent), AU, BE (European patent), CA, CH (European patent), DE (European patent), DK (European patent), ES (European patent), FR (European patent), GB (European patent), GR (European patent), IT (European patent), JP, KR, LU (European patent), MC (European patent), NL (European patent), NO, SE (European patent).

Published

With international search report.

2107586

(54) Title: MICROBURST PRECURSOR DETECTOR UTILIZING MICROWAVE RADAR



## (57) Abstract

A microburst precursor detector utilizes a multiplicity of radar beams (1-4) and samples radar returns, in each beam, from meteorological radar signal reflectors and processes (16) the signal returns in a statistical manner to determine average radar reflectivity and to extract doppler signal parameters. These parameters are utilized to determine a second set of parameters; average doppler frequency within each radar beam, doppler spectral spread within each radar beam, and the skewness of the doppler spectrum in each beam. The second set of parameters is processed (18-20) to establish the existence of a microburst, predicted surface impact, time to impact, wind shear surface location and track, and the magnitude of the wind shear.

MICROBURST PRECURSOR DETECTOR UTILIZING MICROWAVE RADAR  
BACKGROUND OF THE INVENTION

1 1. Field of the Invention

The present invention relates generally to the prediction of weather disturbances and, more particularly, to the prediction of weather disturbances that give rise to microburst wind shear conditions at low altitudes over the earth's surface which are hazardous to aircraft during takeoff and landing.

10 2. Description of the Prior Art

Microburst wind shear is a weather condition which denotes significantly different wind velocities and directions occurring simultaneously at low altitudes over a relatively small region. A microburst wind shear typically lasts 5 to 15 minutes, occurs over a relatively small area, and is extremely hazardous during aircraft takeoffs and landings. Systems of the prior art generally detect microburst ground level wind shear after initial occurrence. In many landing and takeoff situations, these systems do not provide sufficient warning time to permit the avoidance of a wind shear area by aircraft taking off and landing, having provided the danger signal after the onset of the wind shear condition.

25

One method of the prior art for detecting surface wind shear conditions employs ground observations of wind direction and magnitude using mechanical wind sensors at a plurality of locations about an airport. This system has been proven to be inadequate since serious accidents have occurred at airports whereat such systems have been employed due to the untimely or missed detection of the wind shear conditions. A second method utilizes ground based radar. Ground based weather sensing radars typically have narrow antenna beams to enhance moist air detectability and provide high angular resolution.

35

1 A Terminal Doppler Weather Radar, presently in  
development, is intended to detect surface microburst wind  
shear at an airport, as it develops, from a location about  
20 Km from the airport. Such a system is described in the  
5 Proceedings Of The IEEE, vol. 77 no.11, November 1989, New  
York US, pages 1661 -1673. Because of geometric  
considerations, its doppler measurement capability is  
limited to detecting the horizontal movement of  
hydrometers (rain drops) above the earth's surface. It  
10 measures wind shear when there are a sufficient number of  
entrained rain drops to provide a detectable radar echo  
return. It can also measure horizontal movement of  
moisture laden winds aloft which provides indirect  
evidence of the presence of surface microburst wind shear  
15 precursors under some weather conditions. The existence  
of a microburst precursor is established when a descending  
core of high reflectivity with wind convergence at the top  
of the core is detected. The probability of microburst  
precursor detection in this mode is not high and the false  
20 alarm rate, based only on these measurements, will likely  
be unacceptably high.

Other methods of the prior art utilize on-board  
apparatus for detecting the aircraft ground speed and  
comparing this ground speed to the airspeed of the  
25 aircraft. The difference in speeds and the vertical  
aircraft acceleration, determined by inertial sensors,  
provide an indication of the wind conditions about the  
aircraft. Such systems do not provide timely indications  
of wind conditions ahead and, in particular, do not  
30 provide advance warning of microburst wind shear ahead of  
the aircraft. Other prior art on-board wind shear  
detectors provide improved wind shear detection with  
utilization of data provided by the on-board vertical  
accelerometers, true airspeed indicator, pitch angle  
35 indicator, and angle of attack indicator to determine the

# 2107586

-2a-

1 rate of change of vertical wind and thus provide another  
wind shear indicator.

Systems which provide improved surface microburst wind  
shear detection with ground based equipment are disclosed  
5 in U.S. patents 4,649,388 (Re. 33,152) and 4,712,108. The

10

15

20

25

30

35

SUBSTITUTE SHEET

1 invention disclosed in the former patent utilizes a doppler  
radar system with at least two vertically stacked radar  
beams which estimates the surface wind speed doppler  
spectrum of moisture laden air in each vertically stacked  
5 radar beam. If the horizontal wind velocity increases (or  
decreases) monotonically with altitude, the spectral  
components of wind velocity below (above) the point where  
the two spectra are equal are associated with wind  
velocities which occur below (above) the elevation angle  
10 where the two stacked beam patterns cross over. These wind  
speed spectral components provide an estimate of the radial  
doppler velocity resulting from horizontal wind shear as a  
function of range and azimuth, thus permitting the  
detection of the wind shear location and its magnitude. The  
15 invention of the latter patent provides surface microburst  
wind shear detection by processing horizontal doppler radar  
return signals of moisture laden air after the wind shear  
has occurred. By tracking the microburst wind shear center  
in range and azimuth as a function of time, the system  
20 determines the horizontal motion of the microburst wind  
shear centroid, thereby predicting the microburst wind  
shear location during its brief lifetime.

Though these systems may predict the future location of  
25 surface microburst wind shear by tracking a microburst  
after its initial occurrence, they do not have the  
capability, however, of predicting the initial microburst  
wind shear occurrence. Prediction of the future position  
of a microburst after its occurrence does not provide a  
30 warning of wind shear conditions to an airport at the  
initial microburst wind shear location. Another limitation  
of such doppler radar sensors is their inability to detect  
surface microburst wind shear in the presence of very  
little entrained moisture content, a phenomenon which  
35 occurs very often in the western part of the United  
States.

2107586

-4-

1 What is required is a system which reliably predicts the  
location of initial surface microburst wind shear with  
sufficient lead time for safely rerouting an aircraft about  
to land or delaying such landing and takeoffs of aircraft  
5 at that location and will perform this function even when  
there is little moisture in the entrained wind shear  
airflow.

#### SUMMARY OF THE INVENTION

10

It is an objective of this invention to provide adequate  
early warning of a surface microburst wind shear by  
determining a vertical wind downdraft 1-3 Km in diameter  
which precedes the occurrence of surface wind shear by 5 to  
15 15 minutes. The vertical downdraft fans out horizontally  
in all directions when it reaches the ground to generate  
circular or elliptically shaped microburst wind shear.  
This objective is accomplished by detecting the vertical  
wind downdraft during its descent before it reaches ground  
20 level and generates horizontal wind shear. Determination  
of the vertical wind downdraft is accomplished by  
extracting four weather parameters from received signals of  
a scanning single beam or vertically stacked multiple beam  
microwave doppler radar system which illuminates a  
25 preselected altitude range for a predetermined distance  
about an airport. The number of beams of the doppler radar  
system and their beamwidths are designed to provide  
coverage over the preselected altitude range in the  
predetermined region around the airport in a manner that  
30 establishes a vertical or horizontal limit for each range  
cell of the doppler radar system for all slant ranges that  
are less than a predetermined distance. This horizontal  
limit is selected to insure that a vertical wind downdraft  
column completely fills the beam, while the vertical limit  
35 restricts the effects of wind velocity gradients within a  
range cell. The extracted doppler signal weather parameters  
are utilized to establish hydrometer (precipitation)

1 vertical velocity, horizontal velocity, and spatial  
location. These velocity estimates are based on the  
determination of the mean velocity, spectral width and  
skewness of the precipitation doppler velocity spectrum in  
5 each range-azimuth cell, radar determined precipitation  
reflectivity in each range azimuth cell from which the  
radar signal is returned, the azimuthal direction of the  
beam, and the radar beam elevation angle and beamwidth.  
Meteorological characteristics of storm generated  
10 microburst precursors are: a vertical wind downdraft  
velocity of at least five meters per second, a vertical  
wind downdraft column between 1.5 and 3.0 kilometers in  
diameter, and an increase in precipitation reflectivity  
within the vertical wind downdraft of 0-20 dB over that of  
15 the surrounding regions. All of these criteria are  
utilized to confirm that a microburst generating downdraft  
has been initiated.

The received doppler velocity spectrum is the result of  
20 combining the doppler radar determined radial component of  
vertical rain drop velocity, which is a function of the  
sine of the elevation angle, with the radial component of  
horizontal rain drop velocity, which is a function of the  
cosine of the elevation angle, over a relatively wide  
25 vertical antenna beamwidth. The resulting velocity  
spectrum is unique for each combination of average vertical  
and horizontal hydrometer velocities within each range-  
azimuth cell. The measured doppler spectrum parameters in  
each range-azimuth cell in each beam within the illuminated  
30 altitude region are stored on successive radar scans to  
establish a four dimensional parameter map. The doppler  
spectral parameters include mean doppler velocity, doppler  
spectrum width, doppler spectrum asymmetry and total  
spectral power in the radar echo. These measured  
35 parameters of hydrometers immersed in a microburst  
downdraft provide the basic information from which  
microburst precursor vertical and horizontal wind velocity

## 2107586

1 can be estimated. When it is determined from these maps  
that a vertical wind column of between 1.5 and 3.0  
kilometers having a vertical wind velocity which exceeds  
five meters per second and exhibiting a precipitation  
5 reflectivity that is 0-20 dB above the surrounding areas  
has been detected, a microburst warning is generated.  
Since the time for the vertical downdraft to descend to the  
earth's surface is on the order of five minutes, this  
warning will precede the actual occurrence of surface  
10 microburst wind shear by a time that is adequate to divert  
landing aircraft or to delay an aircraft takeoff.

## BRIEF DESCRIPTION OF THE DRAWINGS

15 Figure 1 is a diagram which is useful for explaining  
weather conditions that give rise to a microburst and the  
establishment of wind shear conditions.

Figure 2 illustrates the precursors of a microburst.

20

Figure 3 is an illustration of vertically stacked multiple  
beams that may be employed to obtain microburst prediction  
data.

25 Figure 4 is a block diagram of a preferred embodiment of  
the invention.

Figure 5 is a block diagram of a receiver which may be  
utilized in the preferred embodiment of Figure 4.

30

Figure 6 is a block diagram of a processor which may be  
utilized for the parameter estimator shown in Figure 4.

35 Figure 7 is a block diagram of a processor which may be  
employed for the detection triggers of Figure 4.

1 Figure 8 illustrate processors which may be employed for  
the microburst locator shown in Figure 4.

Figure 9 is a plot of doppler spectral sknewness vs. radial  
5 velocity.

Figure 10 is a plot of doppler spectrum width vs. radial  
velocity.

10 Figure 11 is a block diagram of a processor which may be  
employed as the wind shear predictor in Figure 4.

#### DESCRIPTION OF THE PREFERRED EMBODIMENTS

15 A major cause of aircraft landing/take-off accidents is a  
particular form of wind shear, referred to as a  
microburst. The term microburst, coined to connote an  
aviation hazard, is a powerful downward blast of moist air  
which causes a violent horizontal burst of air in all  
20 directions near ground level. This violent horizontal  
burst creates a horizontal wind velocity differential  
across its center. A microburst is said to have occurred  
when this wind shear is greater than or equal to 10 meters  
per second across a surface region approximately 4 Km in  
25 diameter below 500 meters above ground level (AGL). At low  
altitudes ground radar detection of wind shear is limited  
by ground returns known as clutter and by the fact that in  
many cases much of the (radar echo producing) moisture in  
the downdraft evaporates before it reaches the ground.  
30 Typical clutter levels and airport surveillance radar  
antenna rotation rates at urban airports limit wind shear  
detection to microbursts having precipitation  
reflectivities in the order of 10-20 dBz or greater. If  
clutter were not present, or attenuated when feasible  
35 through signal processing means, noise limitations  
determine detectable signal levels and an order of  
magnitude increase in sensitivity would be realized. The

2107586

-8-

1 degree that clutter can be attenuated through signal  
filtering is dependent on antenna rotation rates and  
azimuth beamwidth. More rapid antenna rotation or narrower  
antenna beamwidths produce higher levels of modulation of  
5 ground clutter making it more difficult to reduce clutter  
through input signal filtering. Two types of microbursts  
are known: dry and wet. Dry microbursts generally occur in  
dry climates whereat heavy rain aloft, which initiates the  
events that cause severe ground wind shear conditions,  
10 mostly evaporates before reaching the ground. Dry  
microburst wind shear, due to the low level of entrained  
moisture at the ground level, exhibit reflectivities well  
below 20 dBz. Wet microburst wind shear generally occurs  
in regions of heavy rain and only partially evaporates  
15 before reaching the ground. Such microburst wind shear  
normally exhibit reflectivities well in excess of the 20  
dBz level. Thus ground clutter inhibits the detection of  
dry microburst wind shear as well as wet microburst wind  
shear by radar systems operating with near ground level  
20 radar beams.

Refer now to Figure 1. A microburst is caused by a strong  
vertical downdraft, having a horizontal diameter D that is  
between 1.5 and 3 kilometers, which originates at high  
25 altitudes. The disturbance diameter increases as the  
downdraft approaches the earth's surface and establishes a  
horizontal wind velocity differential  $V=V_2-(-V_1)$  near the  
surface, that is at least 10 meters per second (20kts) and  
may be between 60kts and 100kts, over a distance W of at  
30 most 4 Km. (When W is greater than 4 Km, a macroburst is  
said to have occurred, a condition which is less dangerous  
for aircraft landing or taking off.) Although a downdraft  
is one of several meteorologically detectable phenomena,  
which are collectively referred to as microburst  
35 precursors, the downdraft is the least unambiguous  
precursor of follow-on surface microburst wind shear.

1 Landing aircraft AC entering a microburst wind shear region  
first experiences an increase in head wind which causes the  
aircraft AC to fly above the glide slope GL. The pilot may  
attempt to return to the glide slope GL by reducing air  
5 speed and angle of attack. As the aircraft AC continues  
through the microburst, it encounters a strong downdraft  
which forces it downward while it moves horizontally and  
then a tail wind resulting in a loss of lift. As the  
aircraft AC falls beneath the glide slope GL, the pilot  
10 must now increase power and angle of attack to bring the  
aircraft AC back to the glide slope GL. Since the aircraft  
requires a finite time to respond to the control commands,  
a crash may occur when it is too close to the ground to  
recover.

15

Microburst precursors occur between 1 and 8 Km above ground  
level (AGL) about 5-15 minutes prior to the onset of low  
altitude wind shear. A diagram depicting the formation of  
a typical wet microburst is shown in Figure 2. In the first  
20 stage 10 a core 11a of densely packed water, with a  
concomitant high reflectivity, is formed at an altitude of  
between 3 and 8 Km AGL. Coinciding with the formation of  
the core 11a is an inflow of air 12a at or above the core  
11a. When instability causes the high reflectivity core  
25 11a to descend, it causes an additional convergence of air  
13a behind its descent and, in many cases, air rotation 14a  
of the descending column. The falling high reflectivity  
core 11a also pushes moisture laden air below it downward,  
resulting in a strong downdraft which accelerates as air  
30 cooling takes place due to moisture evaporation. This high  
reflectivity core may reach the surface coincident with or  
after wind shear has been initiated. The strong downdraft  
establishes an air divergence 17a at the surface, giving  
rise to the wind velocity differential  $V=V_2-V_1$ .

35

Thus weather phenomena aloft provide detectable precursors  
from which microbursts at the surface may be predicted with

2107586

-10-

1 sufficient lead time to prevent an aircraft disaster during  
landing or takeoff. Precursors associated with the  
descending downdraft include: a descending reflectivity  
core, horizontal wind convergence aloft, and horizontal  
5 rotation of the downdraft column. These precursors are  
indirect signatures of the vertical wind downdraft, which  
is the direct cause of surface microburst wind shear. Since  
a descending high reflectivity core together with wind  
convergence and rotation are only indirect signatures of  
10 the vertical wind downdraft, they are less reliable than  
direct measurement of the vertical wind velocity as  
indicators of an impending microburst. Descending high  
reflectivity cores, coupled with substantial horizontal  
wind convergence and rotation, have been observed without  
15 the occurrence of subsequent microburst; and microbursts  
have also occurred in their absence. Consequently,  
unambiguous prediction of a microburst requires direct  
knowledge of a vertically descending downdraft having a  
reflectivity greater than 15 dBz that is typically at least  
20 equal to or greater than the surrounding region, and a  
vertical wind velocity greater than 5 meters per second  
within a column having an aloft diameter between 1.5 and  
3.0 Km. As the moist downdraft descends, evaporation in  
the column causes cooling and induces an acceleration which  
25 can increase the vertical wind velocity up to 25 meters per  
second. The presence of all three factors establishes a  
definite precursor of an imminent microburst.

Consequently, an early warning system for the prediction of  
30 a surface microburst must be able to detect vertical  
downdrafts at altitudes 1-3 Km. This may be accomplished  
with a Doppler radar system having a single beam oriented  
for high elevation angle scanning or having a multiplicity  
of stacked beams, each oriented to scan an assigned  
35 elevation sector, as shown in Figure 3. In a stacked beam  
system, the number of beams and the individual beam widths  
are selected to provide coverage over a desired altitude

1 range AGL in a region around an airport. Once the  
 elevation coverage and the number of beams to provide this  
 coverage is selected, an elevation beam width for each beam  
 is established which provides approximately the same  
 5 percentage spread of vertical wind velocity as measured in  
 each elevation beam.

The elevation beam width for each beam in the beam  
 configuration in Figure 3 would be selected in accordance  
 10 with the following relationship:

$$\frac{\sin \theta_1}{\sin \theta_2} \approx \frac{\sin \theta_2}{\sin \theta_3} \approx \frac{\sin \theta_3}{\sin \theta_4}$$

where  $\theta_n$  are the successive elevation angles defining each  
 15 elevation beam crossover.  $\theta_n$ , shown in Figure 3, is the  
 elevation angle of the nth stacked beam. Though only three  
 beams are shown in Figure 3, this is not restrictive and a  
 greater or lesser number may be chosen to optimize coverage  
 at a system location.

20 Refer now to Figure 4 wherein a block diagram of a  
 preferred embodiment of the invention is shown. Signals  
 received by the stacked beam antenna 11 are coupled to a  
 beam selector 12 wherefrom a selected beam is coupled to a  
 coherent receiver 13. The beams are rotationally selected  
 25 to provide a continuous elevation sector coverage as the  
 antenna 11 is rotated azimuthally by an azimuth drive  
 mechanism 14. As will be explained, coherent receiver 13  
 provides two output signals, designated I and Q to a  
 parameter estimator 15 which includes a doppler spectrum  
 30 mean (average) velocity estimator 15a, a doppler spectrum  
 velocity width (variance) estimator combined with a mean  
 doppler spectrum asymmetry estimator 15b, a reflectivity  
 estimator 15d, a signal-to-clutter estimator 15e and a  
 35 combined reflectivity and S/C comparator 15f. Signals  
 representative of the mean spectral velocity estimate, mean  
 spectral width estimate, mean spectral asymmetry estimate,  
 and the reflectivity estimate obtained from processing the

2107586

-12-

1 I and Q signals are coupled from the parameter estimator 15  
to a parameter mapper 16, which also receives slant range  
representative signals from a range gate generator, not  
shown, antenna azimuth position representative signals from  
5 the antenna azimuth drive mechanism 14, beam selection  
representative signals from the beam selector 12 and a  
gating signal from the comparator 15f when the reflectivity  
estimate and signal/clutter ratio estimate both exceed  
predetermined thresholds.

10

After a gating signal has been received, the four estimate  
representative signals for the N most recent azimuthal  
scans are stored in a mean velocity memory 16a, a velocity  
spectral width memory 16b, an asymmetry memory 16c, and a  
15 reflectivity memory 16d. Stored signals 16a, 16b and 16d  
are coupled to a detection circuit 17, wherein triggers for  
continued processing are generated. A microburst downdraft  
locator and verified 18 processes all four signals stored  
in the parameter mapper 16 to verify the existence and  
20 track of microburst precursors when triggered by signals  
from the detection circuit. The microburst precursor track  
signals are coupled to a wind shear predictor 19 wherein  
the microburst impact location, wind shear magnitude, time  
to impact, and type of microburst (wet or dry) are  
25 determined. Microburst impact location and wet or dry  
microburst information are coupled from the impact location  
predictor 19 to a wind shear tracker 20 which utilize this  
data to provide the wind shear surface track from the  
initial microburst impact location.

30

A schematic diagram of a suitable receiver 13 is shown in  
Figure 5. Signals from the beam selector 12 are coupled  
through a RF filter 13-1 to a mixer 13-2 wherein the  
filtered RF signals, which are within a predetermined  
35 bandwidth about the radar operating frequency, are mixed  
with a signal provided by a stabilized local oscillator  
(STALO) 13-3 to provide intermediate frequency (IF) signals

1 to an IF amplifier 13-4. The bandwidth of the IF amplifier  
is chosen to optimize the signal-to-noise ratio and to  
provide maximum decorrelation between signal samples in  
adjacent range cells. Signals from the IF amplifier are  
5 coupled to an I/Q demodulator 13-5 wherefrom a signal  
component that is in-phase (I) with a signal coupled to the  
I/Q demodulator 13-5 from a coherent oscillator (COHO) 13-6  
is provided on line 13-7, while a signal component that is  
in quadrature (Q) with the COHO signal is provided on line  
10 13-8. The I and Q signals are respectively coupled to  
video amplifiers 13-9 and 13-10 wherefrom the amplified  
analog signals are converted to digital signals in A/D  
converters 13-11 and 13-12, respectively. The I and Q  
digital signals are provided on lines 13-13 and 13-14,  
15 respectively, for further processing and to a noise  
measuring circuit 13-15, wherein the receiver noise is  
determined. This noise measurement may be performed when  
the receiver is initially tested and the noise level noted  
in the system for later use, as will be described  
20 subsequently, or it may be performed at periodic intervals  
to provide an updated noise level and as a receiver check.

Those skilled in the art will recognize that there are two  
general approaches for estimating mean velocity, spectral  
25 width and spectral skewness. One approach is to first  
calculate the power spectrum of the received pulse train in  
each range-azimuth bin using digital signals I and Q and  
then using standard formulas to calculate these  
quantities. The second is to calculate the complex  
30 autocorrelation function of the received signal using  
digital signals I and Q. The second approach is favored  
for the preferred embodiment of the invention since  
estimates of spectral width and spectral skewness will be  
significantly more accurate at low S/N with this approach.

35

The digital I and Q signals are coupled to a dot product  
calculator 15-1, a cross product calculator 15-2, and a

2107586

-14-

1 mean power calculator 15-3 of the parameter estimator 15,  
 as shown in Figure 6. A pulse repetition rate for the radar  
 transmitter is chosen to provide a multiplicity of pulses  
 per range cell which, for example, may be 1600. These  
 5 pulses are processed utilizing a predetermined number of  
 pulse intervals which, for example, may be 1 through 16.  
 The 1 pulse interval is representative of processing that  
 meets the Nyquist criteria for providing unambiguous  
 resulting signals. Pulse intervals greater than 1 are  
 10 representative of processing that does not meet this  
 criteria but are utilized for the sake of significantly  
 improving parameter estimates of mean doppler velocity,  
 doppler velocity spectral width and spectral asymmetry.  
 When 1 pulse interval is utilized, dot product calculator  
 15 15-1 multiplies the I component of a received signal within  
 a given range bin with the I component of the next received  
 signal in that range bin and adds the product so obtained  
 with the product obtained by similarly multiplying the Q  
 component of the received signal with the Q component of  
 20 the next received signal. These summed products may be  
 obtained by multiplying the I and Q components for the  
 first and second received signals, the second and third  
 received signals, the third and fourth received, etc.  
 Summed products may then be averaged over the number of  
 25 product sums to provide a signal representative of an  
 averaged product-sum  $X_1$ . In 2 pulse interval processing,  
 the I and Q components of the first and third received  
 signals are multiplied, the second and fourth received  
 signals are multiplied, and so on to form product-sums,  
 30 which are then averaged to provide a signal representative  
 of a second averaged product-sum  $X_2$ . The average values  $X_m$   
 may be expressed mathematically as:

$$X_m = \frac{1}{N-m} \sum_{n=1}^{M-m} I_n I_{n+m} + Q_n Q_{n+m}$$

$$35 \quad m = 0, 1, 2, \dots, M$$

Note that  $m = 0$  provides an estimate of the average  
 received power in a range bin.

-15-

1 Cross product calculator 15-2 operates in a manner similar  
to that of the dot product calculator 15-1. In this unit,  
however, when one pulse interval processing is utilized,  
the product of the I component of the second received  
5 signal with the Q component of the first received signal is  
subtracted from the product of the I component of the first  
signal with the Q component of the second received signal.  
Such multiplication and subtraction continues with the I  
10 component of the second received signal multiplied with the  
Q component of the third received signal and the I  
component of the third received signal multiplied with the  
Q component of the second received signal, and so on. The  
difference of the paired signal products may then be summed  
and averaged to provide a signal representative of an  
15 averaged cross product  $Y_1$ . When two pulse interval  
processing is utilized, the multiplications are between the  
components of the  $n$ th and the  $n$ th plus two received  
signals. As previously, the differenced products are  
summed and averaged to provide a signal representative of  
20 an averaged cross product  $Y_2$ . The averaged cross products  
 $Y_m$  may be expressed mathematically as:

$$Y_m = \frac{1}{N-m} \sum_{n=1}^{N-m} I_n Q_{n+m} - I_{n+m} Q_n$$

$$m = 1, 2, \dots, M$$

25 Those skilled in the art will recognize that the dot and  
cross products are the real and imaginary parts of the auto  
correlation function for a selected lag value  $m$  of the  
received signals. The products  $X_1$  and  $Y_1$  may be coupled to  
a mean doppler velocity calculator 15-4 wherein an  
30 unambiguous value of the mean doppler velocity  $V$  is  
determined from the following formula:

$$V = \frac{\lambda}{4\pi h} \tan^{-1} \frac{Y_1}{X_1}$$

35 where  $h$  is the sampling period (sampled-pulse interval) and  $\lambda$   
is the radar signal wavelength. Higher order lag products  
 $X_m$  and  $Y_m$  may be utilized to improve the estimate of  $V$  by  
properly removing the velocity ambiguity in  $\tan^{-1}(Y_m/X_m)$

2107586

1 using  $\tan^{-1}(Y_i/X_i)$  as a reference and averaging all  
 estimates. Mean power calculator 15-3 squares and sums the  
 I and Q components for each received signal to determine  
 the power of each received signal and averages the powers  
 5 of all the received signals. This corresponds, as  
 previously noted, to a dot product for which  $m = 0$ . The  
 mean power  $P$  is therefore:

$$P = \frac{1}{N} \sum_{n=1}^N [(I_n)^2 + (Q_n)^2]$$

10

Doppler velocity spectral width  $\sigma$  may be determined from  
 the magnitude of the autocorrelation function at various  
 lags. The generic form is as follows:

$$\sigma^2 = \frac{1}{2\pi^2 h^2 n^2} \frac{|R(mh)| - |R(nh)|}{|R(mh)| - (1/n^2) |R(nh)|} \quad \text{for } m < n$$

15  $n=2, 3, \dots, N$

where  $|R(ah)| = [(X_a)^2 + (Y_a)^2]^{1/2}$

and where  $N$  corresponds to the highest order useful lag  $Nh$   
 ( $N$  is limited by the correlation width of the rain  
 return). While all of the above yield the same value of  $\sigma$ ,  
 20 selected values of  $m$  and  $n$  are either more convenient for  
 calculation or yield more accurate results. The  $\sigma$   
 estimates provided by a set of selected values of  $(m, n)$  are  
 averaged to further improve the estimate accuracy of  $\sigma$ .  
 The sampling rate based on the Nyquist criteria does not  
 25 affect the determination of  $\sigma$ . Thus an unambiguous mean  
 velocity  $\alpha$  and the doppler spectral width  $\sigma$  for the rain  
 are obtained with an economy of memory and processing time.

30 A third parameter necessary for the determination of a  
 microburst precursor may be established by coupling the  
 power representative signal  $P$  from the mean power  
 calculator 15-3 to a mean reflectivity determinator 15-6.  
 Radar reflectivity  $Z$  is related to  $\eta$ , the scatter cross-  
 section per unit volume, by

35

$$\eta = \frac{\pi^5}{\lambda^4} |K_w|^2 Z$$

2107586

-17-

1 Since  $K_w$  is close to unity in the present application,

$$\eta \approx \frac{\pi^5}{\lambda^4} Z$$

The scattering cross-section  $A$  is computed as

5 
$$A = \eta V = \frac{\pi^5}{\lambda^4} Z V$$

where  $V$  is a unit volume of precipitation with radar reflectivity  $Z$ . Knowledge of the power received in a particular range bin together with its range and the radar's operating parameters permits the calculation from the radar equation of  $A$  and  $V$  and therefore  $Z$ . Since the radar parameters and range are known a-priori for each range bin, a look up table can be constructed which permits direct calculation of  $Z$  for each range bin from the power  $P$  measured in that range bin.

Refer again to Figure 4. A signal representative of the estimated reflectivity is coupled from the reflectivity estimator 15c to the comparator 15f wherein it is compared with a signal representative of a threshold reflectivity, which, for example, may be 15 dBz. When the threshold signal in a particular range bin is exceeded, gates 16e, 16f, and 16g are activated and the mean velocity, variance, and reflectivity for the range bin are stored in the memories 16a, 16b, and 16d, respectively; otherwise, a zero is recorded. Memories 16a, 16b and 16d contain stored entries for the last  $N$ , as for example 3, antenna scans. Each entry in the memories is coupled to the detection circuit 17, wherein each is subtracted from each of the corresponding entries for the two previous scans to obtain temporal differences of rain doppler velocity, rain doppler velocity spectral width, and rain reflectivity. Additionally, each range bin entry is subtracted from the corresponding entry for the two previous range bins to obtain spatial differences of the three parameters. Each difference is compared to a predetermined threshold, and if

2107586 -18-

1 the threshold is exceeded, a trigger signal is generated.  
A schematic representation of this processing, in block  
form, is shown in Figure 7. Whenever either of the  
entries in a subtraction is zero, the difference is  
5 defined as zero and does not exceed the threshold.

Since the processing described above is similar for all  
three parameters, only the processing relating to the  
reflectivity R will be discussed with reference to Figure  
10 7. The reflectivity representative signals from the  
reflectivity determinator 15-6 (Figure 6) for each azimuth  
sweep are coupled to a first shift register 17-1 wherein  
each stage of the register corresponds to a range bin  
along the selected azimuth range sweep and to the negative  
15 input terminals of summation networks 17-2 and 17-3.  
Range bin data for successive range sweeps for an antenna  
scan are serially entered in shift register 17-1. When  
the register 17-1 is full, the last stage contains the  
reflectivity data for the first range bin of the first  
20 range sweep and the first stage contains the reflectivity  
data for the last range bin of the last sweep of the  
antenna scan period. At the entry of data for the first  
range bin of the first range sweep on the next scan into  
the first stage of shift register 17-1, all data in the  
25 register shifts one stage and the data in the last stage  
is coupled from the register 17-1 to the first stage of a  
second shift register 17-4 and to the positive input  
terminal of summing network 17-2. Each reflectivity entry  
causes the data to shift one stage in each shift  
30 register. After two complete scans, reflectivity data for  
all range sweeps have been entered into the registers,  
with the data for the first range bin of the first range  
sweep in each of the two previous antenna scans entered  
respectively in the last stage of each register. Upon the  
35 coupling of the first range bin data of the first range  
sweep on the third scan to the shift register 17-1 and the  
summation networks 17-2 and 17-3, the data in the first

-19-

1 range bin of the first range sweep of the two previous  
antenna scans are respectively coupled to the positive  
input terminals of summation networks 17-2 and 17-3. The  
difference signals at the output terminals of the  
5 summation networks are coupled respectively to comparators  
17-5 and 17-6 wherefrom each provides a trigger signal to  
an OR gate 17-7 should the reflectivity difference signal  
exceed a predetermined threshold signal  $R_T$ . This process  
is repeated for each antenna scan.

10

The reflectivity representative signals in each range  
sweep are also coupled to delay line 17-8, wherein the  
signals are delayed for one range bin interval, and to the  
negative inputs of summation networks 17-9 and 17-10.  
15 Signals delayed for one range bin interval in delay line  
17-8 are then coupled to the positive input terminal of  
summation network 17-9, and to delay line 17-11 wherein a  
second delay of one range bin interval is encountered.  
After the second delay the signals are coupled to the  
20 positive input terminal of summation network 17-10. It  
should be apparent that the signals at the positive input  
terminals of the summation networks represent the  
reflectivity data in adjacent range bins for the same  
azimuth sweep and that the signals at the output terminals  
25 of summation networks 17-9 and 17-10 are the differences  
between the reflectivity representative signals for  
adjacent range bins and between reflectivity  
representative signals for two range bins separated by one  
range bin. These difference signals are respectively  
30 coupled to comparators 17-11 and 17-12 wherefrom trigger  
signals are coupled to OR gate 17-13 when the difference  
signals exceed a second reflectivity representative  
threshold signal  $R_{RT}$ . Trigger signals for the doppler  
velocity  $V$  and doppler velocity spectral width are  
35 generated in a similar manner. In this manner six  
possible triggers (one spatial and one temporal for each  
of the three parameters) may appear at the output  
terminals a-f of OR gates 17a-17f.

2107586

-20-

1 Output terminals a-f are coupled to an OR gate 18-1 of  
microburst downdraft verifier 18a, as shown in Figure 8.  
Thus, if anyone of the six triggers are generated, OR gate  
18-1 couples an enable signal to an elevation beam/sector  
5 search region determinator 18-2. Upon reception of the  
enable signal, the region determinator 18-2 identifies a  
region in which at least one trigger has been generated  
and provides an enable signal to vertical rain velocity  
and horizontal wind velocity estimator 18-3. Upon  
10 reception of this enable signal, estimator 18-3 commences  
processing of the signals within the identified elevation  
beam/sector search region coupled thereto from the memory  
16. Though not shown in the figure, it should be  
understood that the processing is performed in all three  
15 radar beams.

The values of  $V$ ,  $\sigma$ ,  $\beta$ , and  $R$  for each range cell within  
the search region are coupled to a vertical rain velocity  
estimator 18-3, while the coordinates of each range cell  
20 within the search region are coupled via a gate 18-9 to a  
precursor region identifier 18-4. Stored in vertical rain  
velocity estimator 18-3 are pre-calculated data which  
permit estimates of the vertical and horizontal raindrop  
velocity in the downdraft to be determined from estimated  
25 quantities  $V_p$ ,  $\sigma$  and  $\beta$ . The vertical and horizontal  
velocity of the falling precipitation are uniquely related  
within each elevation beam to a 3 parameter set consisting  
of mean doppler velocity  $V$ , doppler spectral width  $\alpha$ , and  
doppler spectral asymmetry  $b$ . This is a result of the  
30 fact that a doppler radar measures the vertical velocity  
component  $V_v$  of the raindrops multiplied by the sine of  
the elevation angle  $\theta$  within an elevation beam while the  
horizontal velocity component  $V_h$  of the raindrops couple  
into the radar doppler measurement multiplied by the  
35 cosine of the elevation angle  $\theta$ .

In elevation beam 1,  $\theta$  varies from  $87^\circ$  to  $47^\circ$ .  
Hence, contributions to the doppler spectrum by the

-21-

1 vertical velocity raindrop component  $V_v$  are multiplied by  
values varying from  $\sin 87^\circ$  through  $\sin 47^\circ$  across the  
elevation beam. Similarly, the raindrop horizontal  
velocity  $V_H$  contributions to the doppler spectrum are  
5 multiplied by values varying from  $\cos 87^\circ$  through  $\cos$   
 $47^\circ$ . The measured doppler spectrum is the sum of both  $V_v$   
 $\sin \theta$  and  $V_H \cos \theta$  contributions. As a result, the three  
parameter set of mean doppler spectral velocity, doppler  
spectral width and doppler spectral asymmetry,  $\{V, r, b\}$  is  
10 a unique function of the vertical and horizontal raindrop  
velocities  $\{V_v, V_H\}$ . For a particular combination of  
raindrop vertical and horizontal velocity  $\{V_v, V_H\}$ , either  
the paired measurement set  $\{V, \alpha\}$  or the paired measurement  
set  $\{V, \beta\}$  is sufficient to uniquely estimate  $\{V_v, V_H\}$ . By  
15 utilizing both paired relationships, accuracy is  
significantly improved. The above explanation also  
applies to elevation beams 2 and 3 except that  $\{V_v, V_H\}$   
have different relationships to  $\{V, \alpha\}$  and  $\{V, \beta\}$ , as a  
result of the different elevation angle coverage within  
20 each elevation beam. Because the above paired  
relationships are the direct result of radar beam  
geometry, they can be pre-calculated and stored in  
vertical and horizontal velocity estimator 18-3 for each  
elevation beam. Typical curves which relate  $\{V, \beta\}$  to  
25 raindrop vertical and horizontal velocity  $\{V_v, V_H\}$  and  
which relate  $\{V, \alpha\}$  to  $\{V_v, V_H\}$  for a typical elevation beam  
are shown in Figures 9 and 10, respectively.

An examination of Figure 9 indicates a region 20 where a  
30 pair of radial velocity and skewness values do not lead to  
a unique set of  $\{V_v, V_H\}$  values. Characteristics of a  
microburst may be utilized to resolve these ambiguities.  
Due to frictional effects of the surrounding air on the  
vertical velocity, the downdraft velocities in a  
35 microburst are slower at the edges than they are at the  
center of the microburst. These frictional forces have no  
effect on the horizontal velocities. Consequently the  
horizontal velocities remain constant across the

2107586

-22-

1 downdraft. In a preferred embodiment of the invention a  
typical microburst extends across 5-to-10, 300 meter wide,  
range bins in a range sweep. A set of radial velocity-  
skewness values is determined for of each of these range  
5 bins. Though some variation in  $V_H$  may exist between range  
bins, only one value of  $V_H$  exists for a paired value of  
radial velocity-skewness in each range bin for any one  
range sweep. This value of  $V_H$  may be determined from plot  
of spectral width vs radial velocity shown in Figure 10.  
10 Once the horizontal velocity is determined in a range bin  
it may be used to determine the vertical velocity in that  
range bin from the skewness-radial velocity plot shown in  
Figure 10, thereby establishing unique values for  $V_v$  and  
 $V_H$ .

15

It should be understood that other methods of resolving  
the ambiguity exist. For example, after  $V_H$  has been  
established in each range bin from Figure 10, the  $V_H$   
values may be averaged and the averaged value used in  
20 Figure 9 to establish  $V_v$ .

Another method for resolving the ambiguity employes the  
relationship to calculate  $V_v$ :

25

$$V_{RAD} = V_v \sin\theta_e + V_H \cos\theta_e$$

where  $\theta_e$  is known for each beam,  $V_{RAD}$  is the estimated  
average doppler for each range bin, and  $V_H$  is determined  
by one of the two above described methods. This approach  
30 may provide a more accurate estimate of  $V_v$  for each range  
bin of the range sweep than either of the methods  
previously described.

Another method of estimating the vertical velocity  $V_v$ , one  
35 which may provide still greater accuracy and also  
establish confirmation of a microburst downdraft  
precursor, utilizes Figure 10 and the known standard

1 deviation of raindrop turbulence in a microburst  
downdraft. A typical microburst downdraft is  
characterized by raindrop turbulence with a standard  
deviation of substantially 1 meter per second. The curves  
5 of Figure 10 are based on this value. If the turbulence  
standard deviation is greater than some pre-established  
value, as for example, 2 meters per second, it is  
determined that the downdraft is not a microburst  
precursor. Since  $V_H$  is constant across the downdraft, a  
10 plot of spectral width vs radial velocity for the range  
bins spanning the microburst define the slope of a  
constant  $V_H$  curve. If a slope for the spectral width vs  
radial velocity curve, significantly greater than the  
slope in a corresponding a region of Figure 10 is  
15 obtained from the data, a turbulence standard deviation  
that is greater than 1 meter per second is indicated. The  
measured slope is a direct measure of the standard  
deviation.

It is straight forward to replace the curves of Figure 10  
20 with plots having a higher value of turbulence standard  
deviation. The revised plot may then be used to estimate  
 $V_V$  and  $V_H$  for each range bin. Such revised curves may be  
used to obtain a separate estimate of  $V_H$  for each range  
bin spanning the downdraft. These estimate values of  $V_H$   
25 may then be averaged to increase the estimate accuracy of  
 $V_H$ . The averaged value of  $V_H$  with the measured value of  
 $V_{RAD}$  in each range bin can be substituted into the  
previous equation to obtain a direct estimate of  $V_V$  in  
each range bin.

30

In order to increase the estimation accuracy of  $V_V$  and  $V_H$ ,  
it is desirable to increase the number of processed pulses  
in each range bin, as for example, from 1600 pulses to  
64,000 pulses, in the microburst search region. While  
35 there are many ways this can be done, one way is to reduce  
the transmitted pulse length, as for example, from 2  
microseconds to .05 microseconds with no change in pulse  
repetition frequency, and sampling I and Q in the receiver

2107586

-24-

1 every .05 microseconds instead of every 2 microseconds.  
This generates 40 range bins where there was previously  
one range bin. The 1600 pulses received in each of the  
forty .05 microsecond range bins are sequentially stacked  
5 to comprise a 64,000 pulse return over a 2 microsecond  
range interval where previously there was only one 1600  
pulse return. The 1600 pulse return from rain in each .05  
microsecond range bin is statistically independent of the  
rain return in all the other range bins. The increase in  
10 the number of processed pulses from 1600 to 64,000, a  
factor of 40, reduces the variance of the estimates of R,  
V,  $\sigma$  and  $\beta$  by 40. This significantly improves the  
estimates of  $V_v$  and  $V_H$ . The processing change has no  
effect on the relations between  $\{V, \sigma, \beta\}$  and  $\{V_v, V_H\}$  shown  
15 in Figures 9 and 10.

Precipitation vertical velocity in still air is a function  
of raindrop size. The radar reflectivity of precipitation  
is also a function of raindrop size. It has been shown by  
20 Joss and Waldvogel ("Raindrop Size Distribution and  
Doppler Velocities," 14th Radar Meteorology Conference,  
American Meteorological Society, Nov/17-20/70) that when  
both quantities are measured simultaneously in the absence  
of wind by a doppler radar, they are empirically related  
25 by

$$v = 2.6 Z^{0.107}$$

where v is doppler radar measured vertical velocity and Z  
30 is precipitation radar reflectivity.

Refer again to Figure 8. Measured reflectivity R in the  
search region is coupled to vertical rain velocity in  
still air estimator 18-5 wherein the Joss-Waldvogel  
35 relationship is utilized to obtain an estimate of the  
vertical rain velocity in still air. This estimate is  
coupled to a differencing network 18-6, wherein it is  
subtracted from the vertical rain velocity estimate,

2107586

-25-

1 coupled to the differencing network 18-6 from the vertical  
rain velocity and horizontal wind estimator 18-3, to  
obtain the vertical wind velocity  $V_{vw}$ .

5 This vertical wind velocity is compared to a threshold  
downdraft velocity  $V_{wt}$ , which is representative of a  
minimum downdraft velocity of a microburst, in a  
comparator 18-7 wherefrom a signal is coupled to enable  
the gate 18-9; thereby providing the address of the range  
10 bins in which the downdraft velocity exceeds the threshold  
to the precursor region identifier 18-4. These addresses  
are stored in the region identifier 18-4 wherefrom they  
are coupled to gate 18-8 and to a spatial extent tester 18-  
10, wherein the spatial extent of the downdraft velocity  
15 exceeding the threshold is determined and compared to a  
stored spatial extent of a microburst. Should the  
comparison determine that the spatial extent of the  
downdraft velocity exceeding the threshold is comparable  
to that of a microburst, gate 18-8 is activated and the  
20 values of vertical and horizontal wind velocity,  
reflectivity, and location are provided at the output  
terminals of the gate 18-8.

The horizontal and vertical wind velocities, reflectivity,  
25 and location coordinates coupled through gate 18-8 are  
provided to the wind shear predictor 19 (Figure 4), a  
block diagram of which is shown in Figure 11. The  
reflectivity is coupled to a microburst predictor 19-1  
wherein a prediction of a wet or dry microburst, based  
30 upon the magnitude of the reflectivity, is made. A dry  
microburst is predicted should  $R$  be between 15-25 dBz and  
a wet microburst is predicted should  $R$  be above 25 dBz.

Horizontal wind velocity provided from the horizontal wind  
35 velocity estimator 18-3, the vertical wind velocity  
provided from the differencing network 18-6, and the  
coordinates of the region in which the downdraft exceeds  
the threshold are coupled to a microburst surface location

2107586

-26-

1 predictor 19-2 which utilizes this data in a conventional  
manner to predict the surface location of the microburst  
impact. The highest vertical wind velocity in the  
downdraft region is also coupled to a time to impact  
5 predictor which, in a conventional manner, predicts the  
time that the microburst will impact the surface and to a  
wind shear magnitude predictor 19-4.

Wet/dry microburst predictor 19-1 and surface location  
10 predictor 19-2 each couple data to the wind shear tracker  
21, which also receives radar data from a radar receiver  
(not shown) that is coupled to a doppler radar beam which  
provides coverage near ground level, beam 4 in Figure 3.  
The wet/dry microburst data, the predicted microburst  
15 impact location, and the data provided by the receiver  
coupled to beam 4 are utilized to track the wind shear  
along the surface and provide predictions of subsequent  
wind shear locations.

20 Dry microburst surface wind shear contains a very small  
amount of moisture, since most of the original moisture  
content aloft evaporates before the downdraft reaches the  
surface. As a result it is very difficult to detect a dry  
microburst wind shear during its earliest occurrence at  
25 ground level because of ground clutter, without the  
predicted microburst downdraft impact location and wind  
shear magnitude. Using information from the wet/dry  
microburst predictor, the time-to-impact predictor, and  
the microburst surface location predictor, the receiver  
30 coupled to beam 4 searches the range-azimuth bins covering  
the predicted surface impact area on each scan to pick up  
the first indications of wind shear resulting from the  
downdraft reaching the ground. After initial detection of  
the wind shear, beam 4 derived information provides up-to-  
35 date information with respect to the location and  
magnitude of microburst wind shear. This information is  
provided until the wind shear magnitude attenuates to the  
point at which it is no longer a treat.

1 While the invention has been described in its preferred  
embodiments, it is to be understood that the words which  
have been used are words of description rather than of  
limitation and that changes within the purview of the  
5 appended claims may be made without departure from the true  
scope and spirit of the invention in its broader aspects.

10

15

20

25

30

35

The embodiments of the invention in which an exclusive property or privilege is claimed are defined as follows:-

1. A method for predicting microbursts comprising the steps of:

radiating radar signals in a plurality of radar beams, each beam providing radar surveillance in a respective elevation angular sector;

receiving radar signal returns in each beam from meteorological radar scatters;

processing said radar signal returns to determine doppler frequency spectrum parameters generated for each radar beam of said plurality of radar beams, to determine average signal-to-clutter ratio of said radar signal returns, and to determine average radar reflectivity of meteorological scatters in each radar beam of said plurality of radar beams;

comparing said average signal-to-clutter ratio to a predetermined threshold;

comparing said average reflectivity with a reflectivity value associated with a microburst;

providing a first enabling signal to first gate means when said average signal-to-clutter ratio exceeds said predetermined threshold and said average reflectivity exceeds said reflectivity value;

coupling said doppler frequency spectrum parameters via said first gate means to processor means; and

processing said doppler spectrum parameters and said average reflectivity determined from said radar signal returns in each beam of said plurality of radar beams for which said enabling signal is provided in said processor means to establish whether a microburst precursor is present.

2. A method in accordance with claim 1 wherein said doppler frequency spectrum parameters and average reflectivity processing step further includes the steps of:

determining location parameters of said vertical wind velocity;

coupling said location parameters to second gate means;

comparing said vertical wind velocity to a predetermined vertical wind velocity and providing a second enabling signal to said second gate means when said vertical wind velocity exceeds said predetermined vertical wind velocity;

coupling said location parameters via said second gate means to spatial extent means for determining spatial extent of said vertical wind velocity;

comparing said spatial extent to a predetermined spatial extent associated with a microburst and providing a third enabling signal when said spatial extent exceeds said predetermined spatial extent;

coupling said third enabling signal to third gate means; and

coupling said vertical wind velocity, said horizontal velocity, said average radar reflectivity and said location parameters via said third gate means to microburst processor means for providing microburst type, time to impact of microburst, surface location and track of predicted wind shear, and predicted shear magnitude.

3. A method in accordance with claim 1 wherein said doppler frequency spectrum parameters and average reflectivity processing step further includes the steps of:

determining average doppler frequency from said doppler frequency spectrum parameters;

determining spectrum skewness from said doppler frequency spectrum parameters; and

determining a spectral width from said doppler frequency spectrum parameters; and

wherein said method for predicting weather disturbances further includes the step of utilizing said average doppler frequency, said spectrum skewness, said spectral width, and said average radar reflectivity to determine vertical and horizontal wind velocities.

4. A method in accordance with claim 3 wherein said utilizing step includes the steps of:

determining vertical rain velocity from said average doppler frequency, said spectrum skewness, said spectral width, and said average reflectivity;

establishing a vertical rain velocity in still air from said average radar reflectivity; and

subtracting said vertical rain velocity in still air from said vertical rain velocity to determine vertical wind velocity.

5. A method in accordance with claim 4 wherein said doppler frequency spectrum parameters and average reflectivity processing step further includes the steps of:

determining location parameters of said vertical wind velocity and coupling said location parameters to second gate means;

comparing said vertical wind velocity to a predetermined vertical wind velocity and providing a second enabling signal to said second gate means when said vertical wind velocity exceeds said predetermined vertical wind velocity;

coupling said location parameters via said second gate means to spatial extent means for determining spatial extent of said vertical wind velocity;

2107586

comparing said spatial extent to a predetermined spatial extent associated with a microburst and providing a third enabling signal when said spatial extent exceeds said predetermined spatial extent;

coupling said third enabling signal to third gate means; and

coupling said vertical wind velocity, said horizontal velocity, said average radar reflectivity and said location parameters via said third gate means to microburst processor means for providing microburst type, time to impact of microburst, surface location and track of predicted wind shear, and predicted shear magnitude.

6. An apparatus for predicting weather disturbances comprising:

means for radiating radar signals in a plurality of radar beams, each beam providing radar surveillance in a respective elevation angular sector;

receiver means coupled to said radiation means for receiving radar signal returns in each beam from meteorological radar scatterers;

estimator means responsive to said radar signal returns for providing estimated doppler frequency spectrum parameters generated for each radar beam, estimated average signal-to-clutter ratio of said radar signal returns in each radar beam, and estimated average radar reflectivity of said meteorological scatterers in each radar beam;

comparator means for comparing said estimated average signal-to-clutter ratio to a predetermined threshold and said estimated average reflectivity of said meteorological scatterers to a predetermined reflectivity value, and providing an enable signal when said estimated average signal-to-clutter ratio exceeds said predetermined

threshold and said estimated average reflectivity exceeds said predetermined reflectivity value;

memory means coupled to said comparator means and said estimator means for storing said doppler frequency spectrum parameters and said estimated average reflectivity when said enabling signal is received;

detection means coupled to said memory means for determining spatial and temporal differences between said stored doppler frequency spectrum parameters and said stored estimated average reflectivities and for providing a trigger when a spatial or temporal difference of a stored doppler frequency parameter exceeds a specified threshold;

locator means coupled to said memory means and said detection means, enabled when one or more triggers are received from said detection means, for processing said doppler frequency spectrum parameters and said estimated average reflectivities to determine an existence of a microburst precursor and for providing precursor tracking signals when existence of a microburst precursor has been established; and

predictor means coupled to receive said precursor tracking signals for providing signals representative of a microburst impact location, wind shear magnitude at said impact location, time to impact, and type of microburst.

7. An apparatus in accordance with claim 6 further including tracker means coupled to receive said microburst impact location for providing a wind shear surface track utilizing said impact location as an initial location.

8. An apparatus in accordance with claim 6 wherein said receiver provides I and Q components of radar return signals, said I component being in phase with a reference signal and said Q component being in quadrature with said reference signal and wherein said estimator means includes:

means coupled to receive said I and Q components of radar signal returns for providing an average dot products of selected pairs of received radar signal returns, each pair having first and second signals, a dot product of a selected pair of radar signal returns being a sum of products of I components and Q components of signals in said selected pair;

means coupled to receive said I and Q components of radar signal returns for providing an average of cross products of said selected pairs of received radar signal returns, a cross product of a selected pair of radar signal returns being a sum of products formed by multiplying said I component of said first signal in said selected pair by said Q component of said second signal in said selected pair and multiplying said Q component of said first signal in said selected pair by said I component of said second signal in said selected pair;

means coupled to said dot product means and said cross product means and responsive to said average of dot products of a first set of selected pairs of doppler signal returns and said average of cross products of a second set of selected pairs of doppler signal returns for providing mean doppler velocity and doppler spectrum asymmetry; and

means coupled to said dot product means and said cross product means and responsive to said average of cross products of said first set of selected pairs and said average of dot products of said second set of selected pairs for providing doppler velocity spectral width.

9. An apparatus in accordance with claim 6 wherein said locator means includes:

region identifying means coupled to said detection means and enabled by said trigger for identifying spatial regions wherein a spatial or temporal difference for at least one doppler parameter exceeds said specified threshold and for providing enabling signals during radar surveillance of identified spatial regions; and

means coupled to said memory means to receive doppler frequency parameters in said identified spatial regions and to said region identifying means for providing vertical wind velocity in said identified spatial regions, horizontal wind velocity in said identified spatial regions, and said average reflectivity in said identified spatial regions to said predictor means.

R. WILLIAM WRAY & ASSOCIATES  
BOX 2760 - STATION D  
OTTAWA, CANADA K1P 5W8  
PATENT AGENT FOR THE APPLICANT

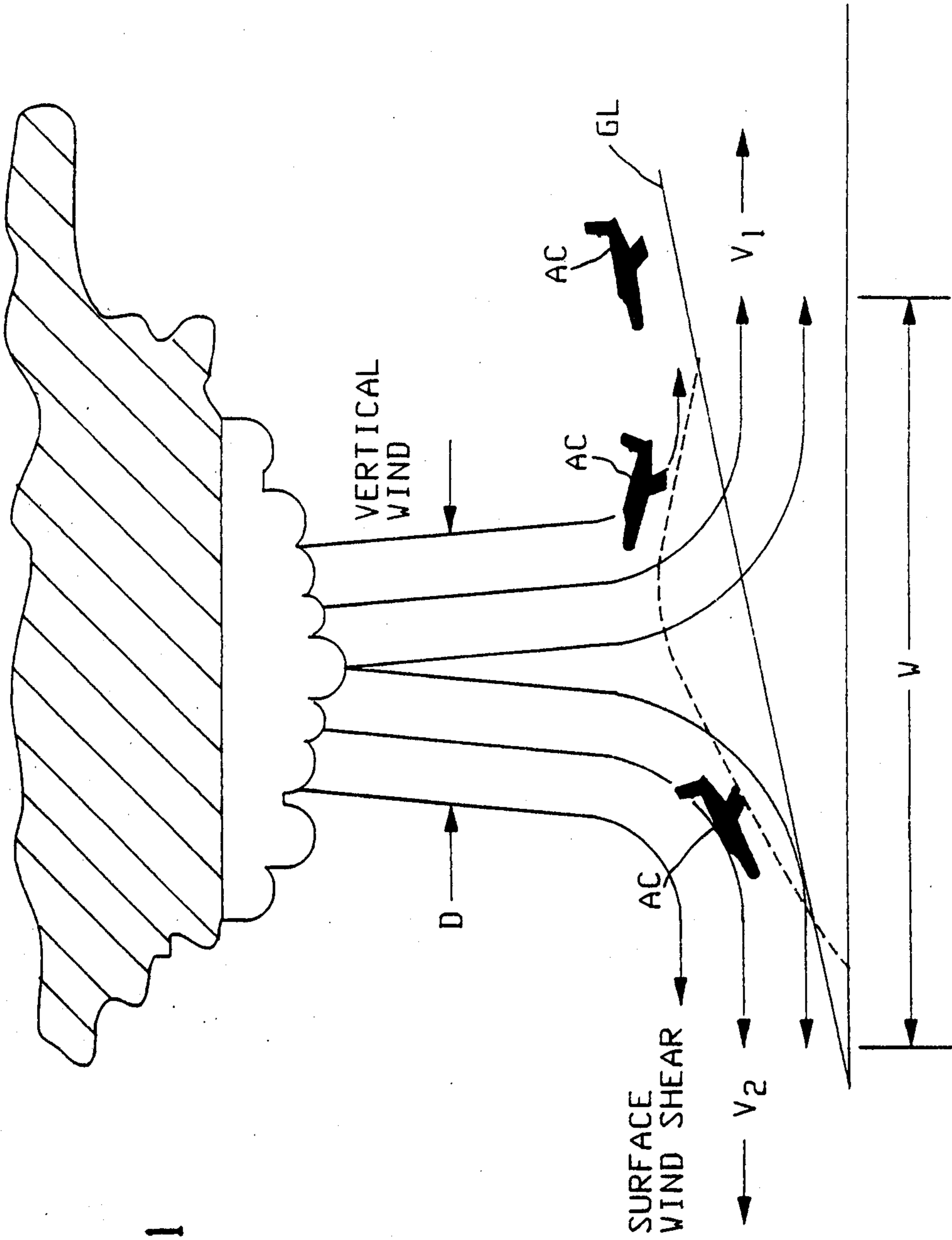
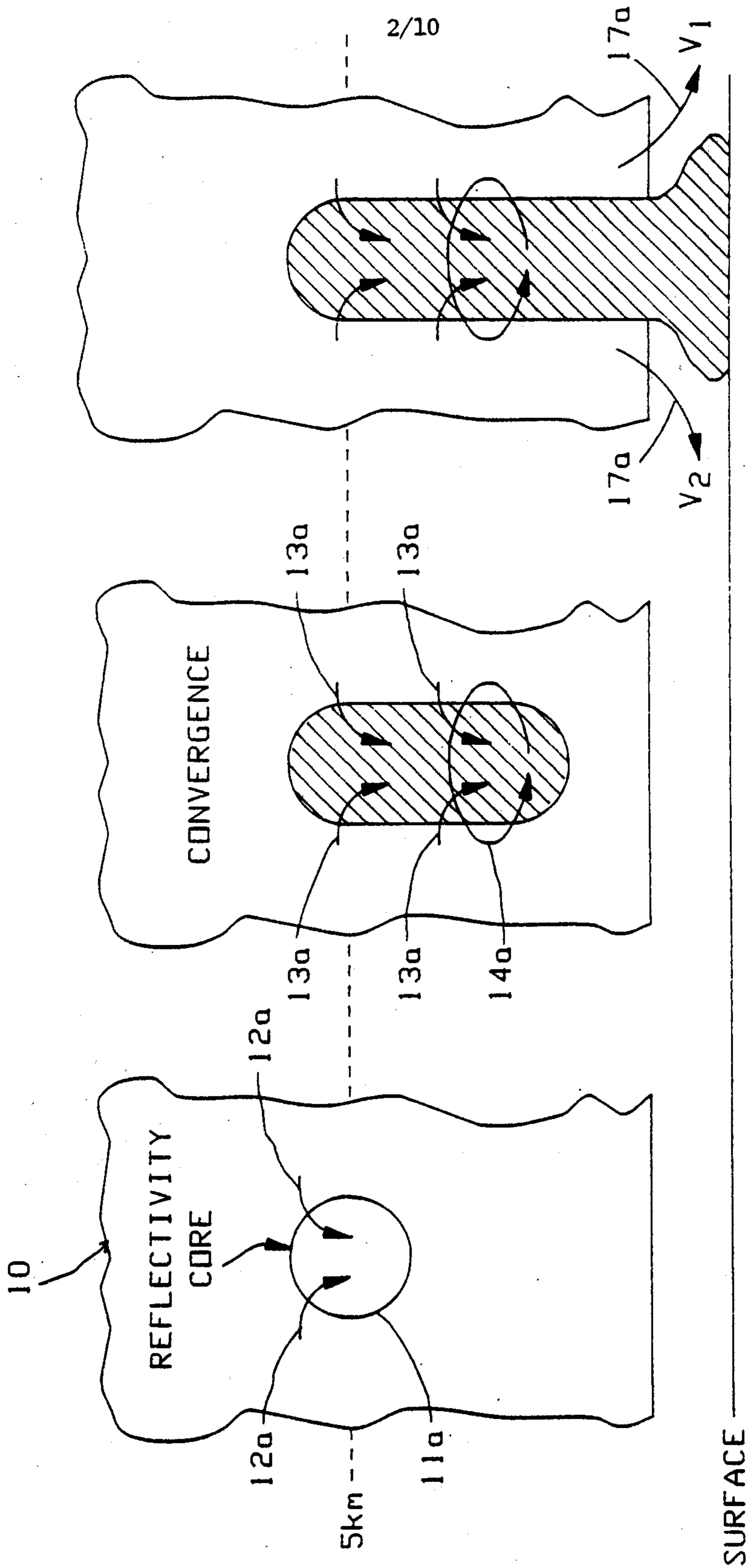


FIG. 1

FIG. 2



2107586

3/10

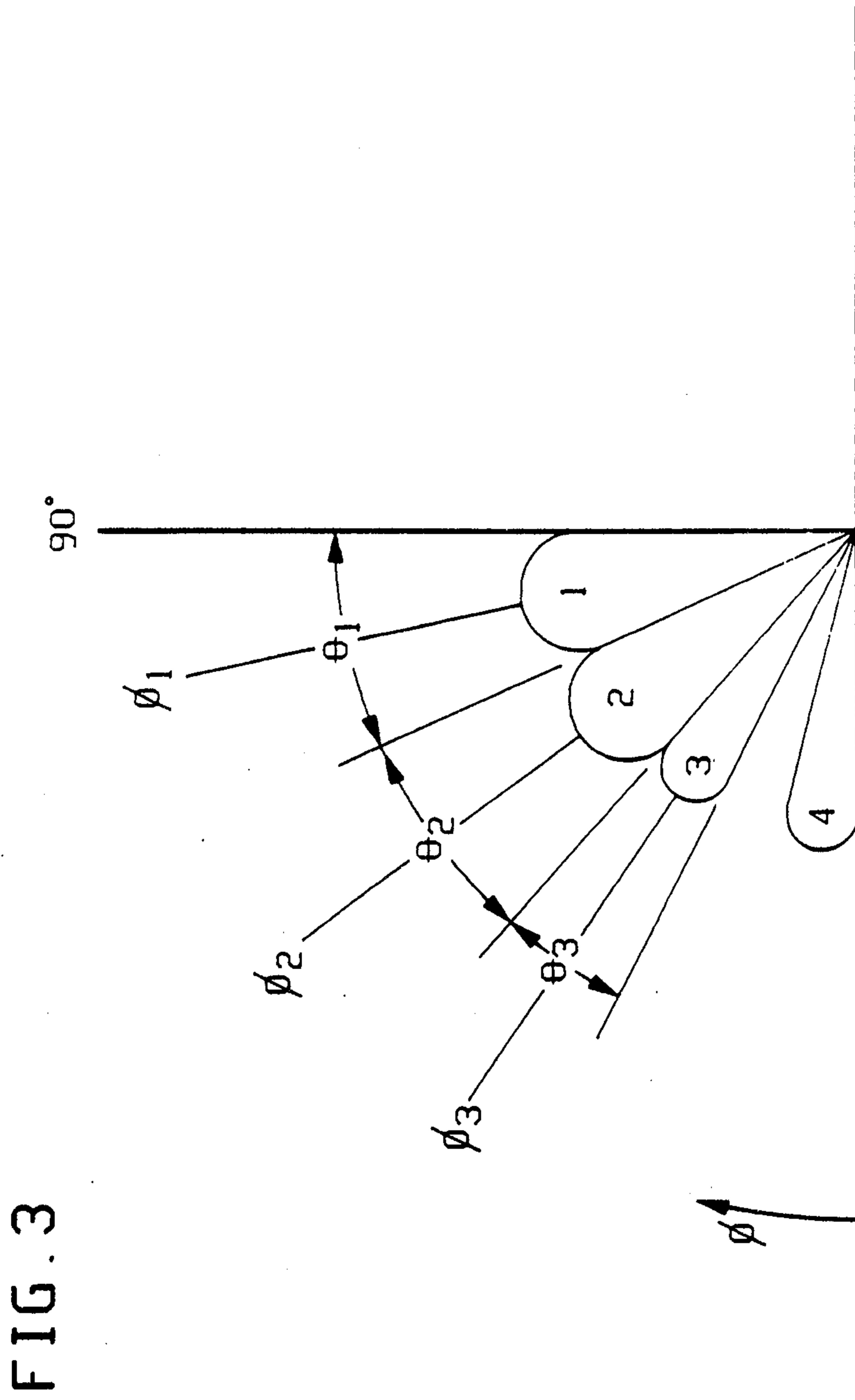


FIG. 3

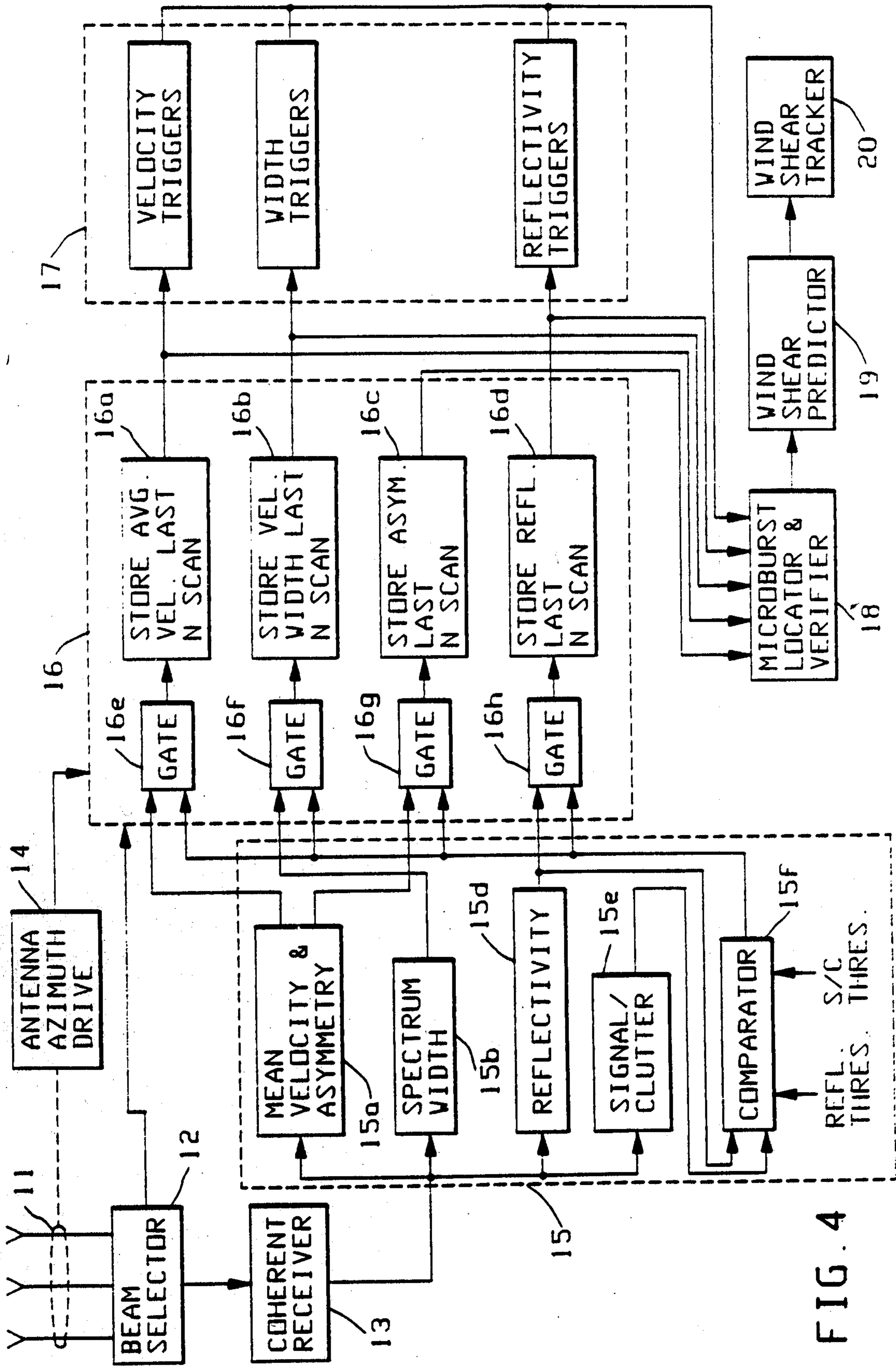


FIG. 4

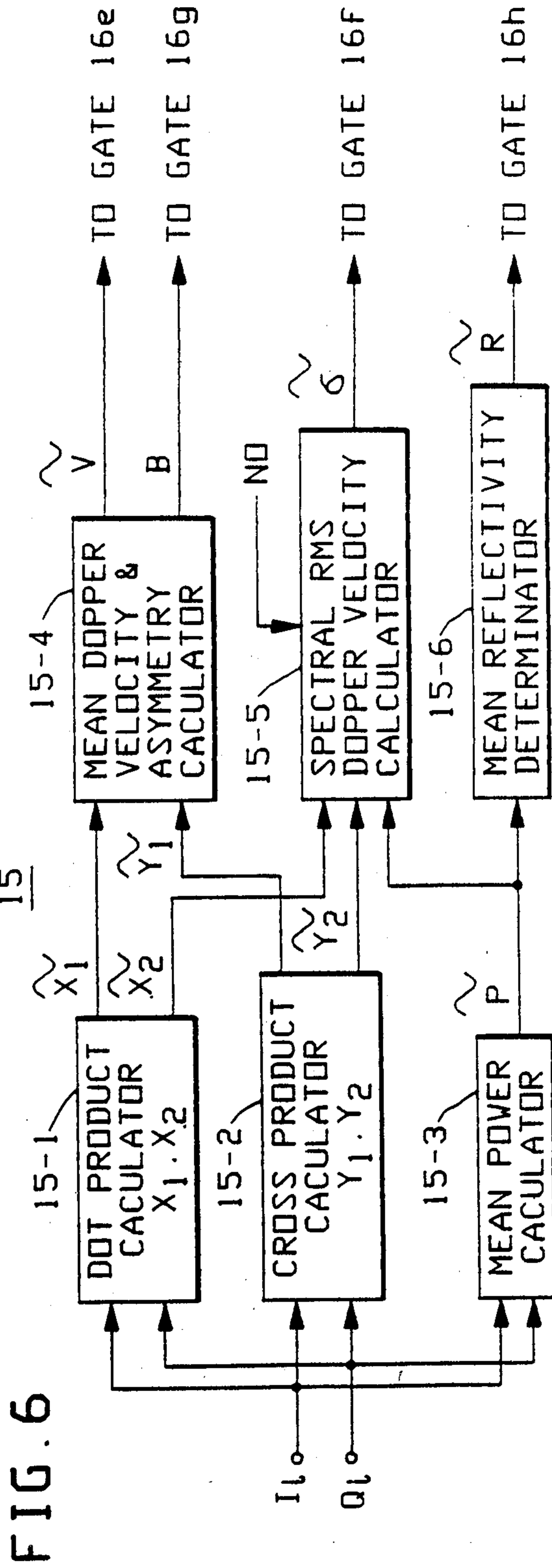
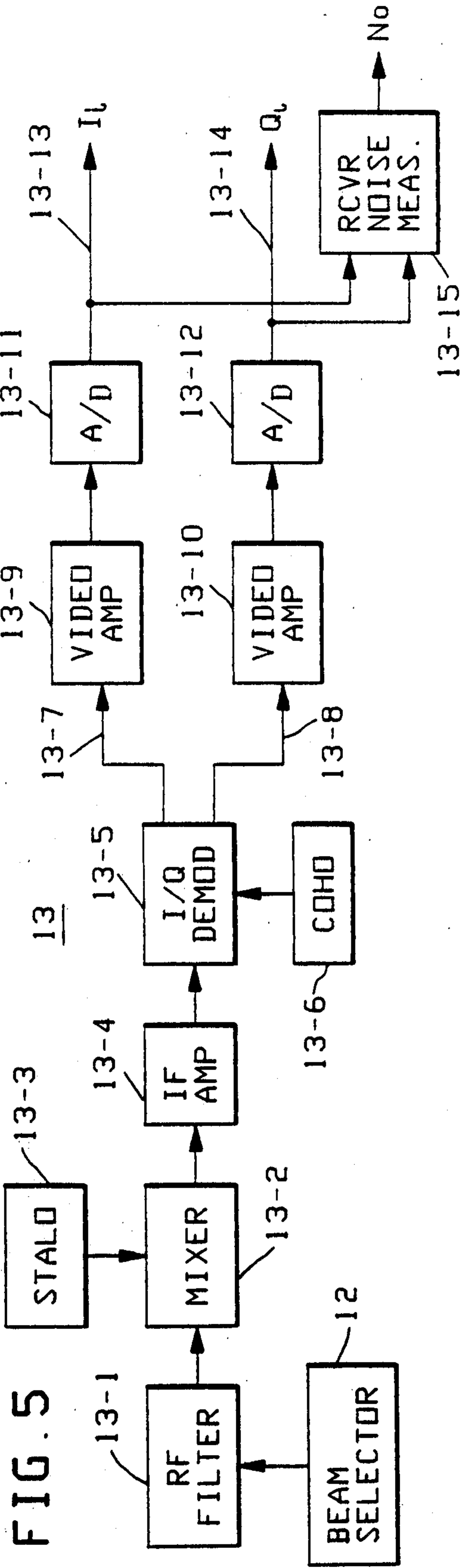


FIG. 5

FIG. 6

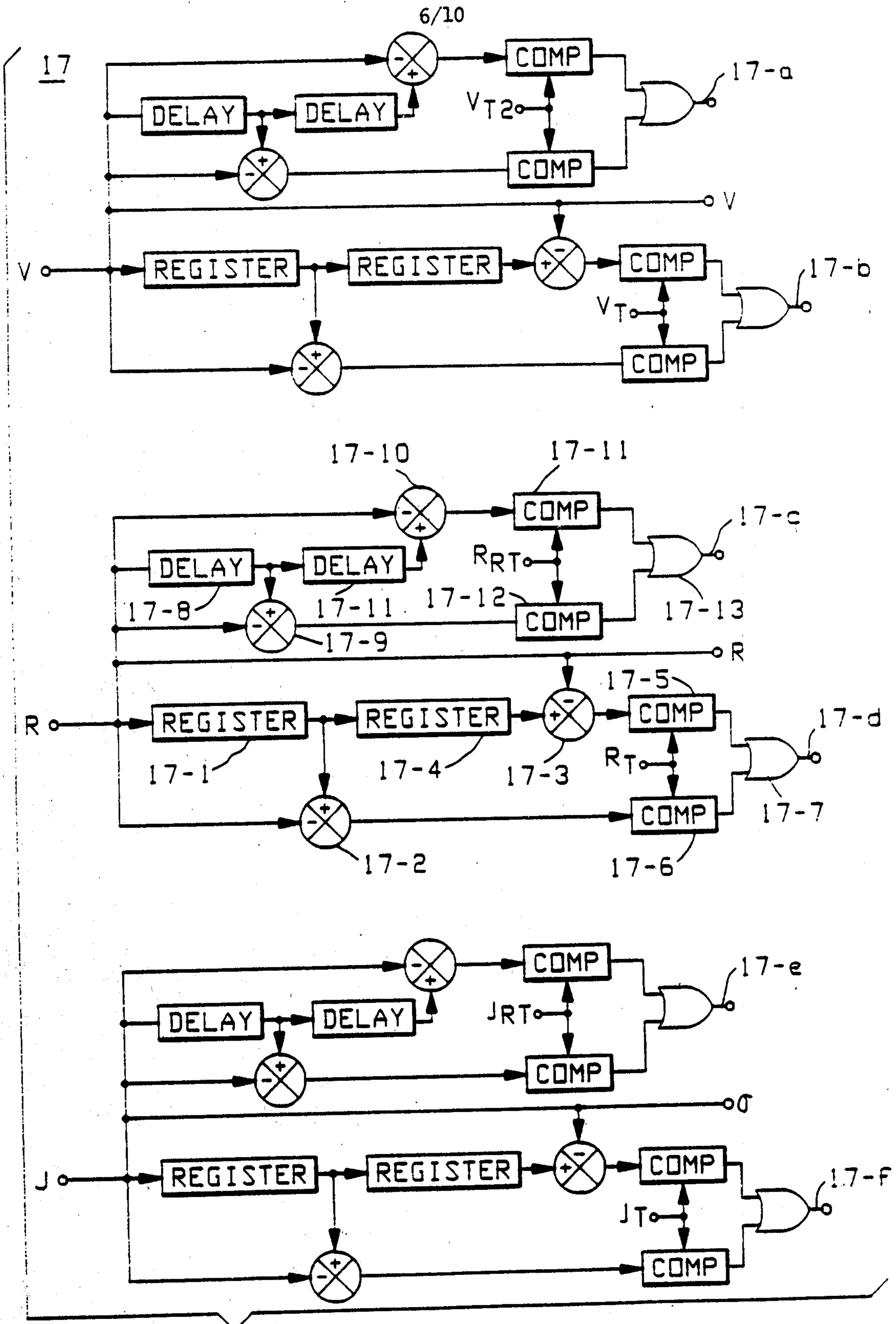
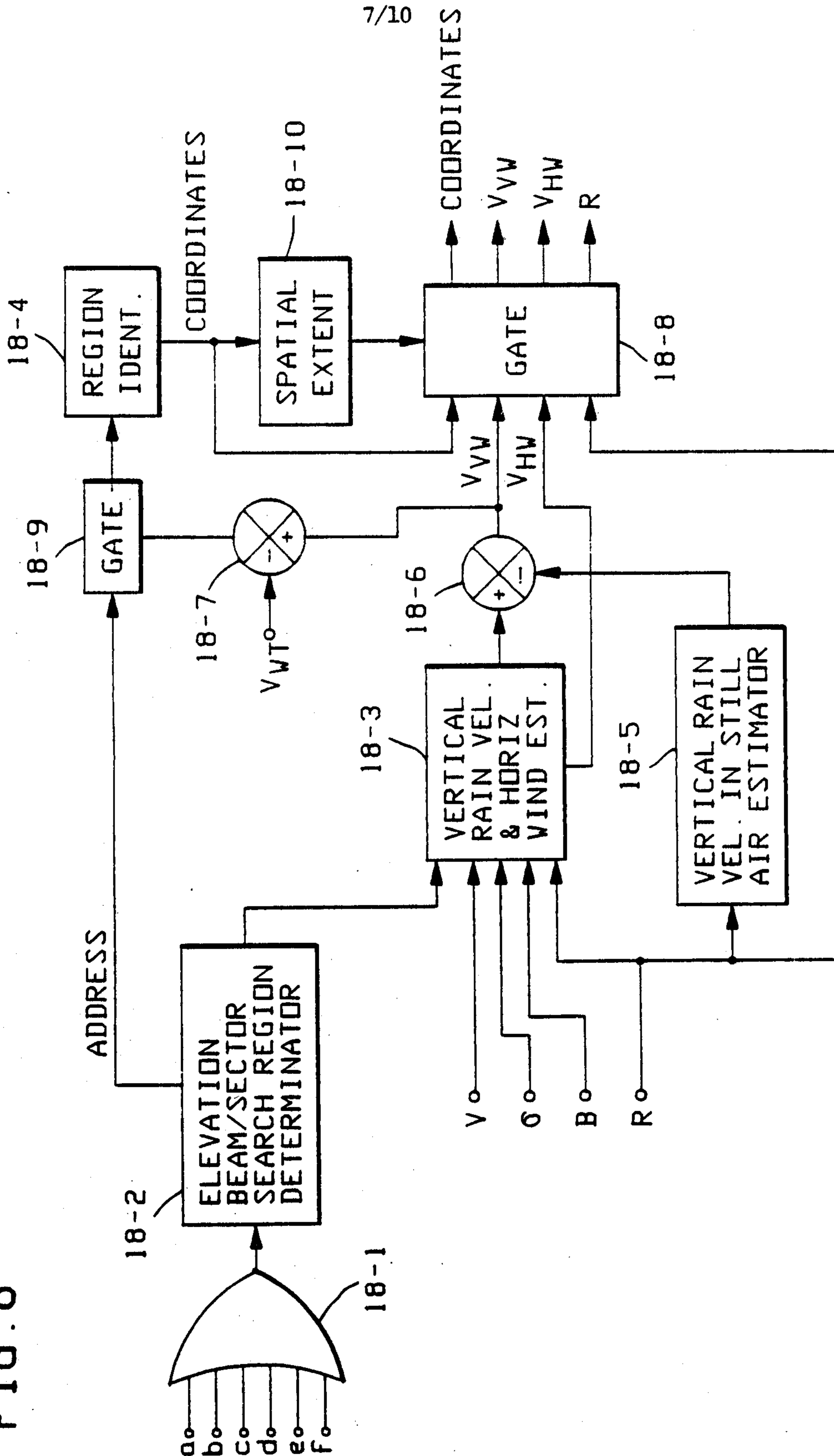


FIG. 7

7/10

FIG. 8



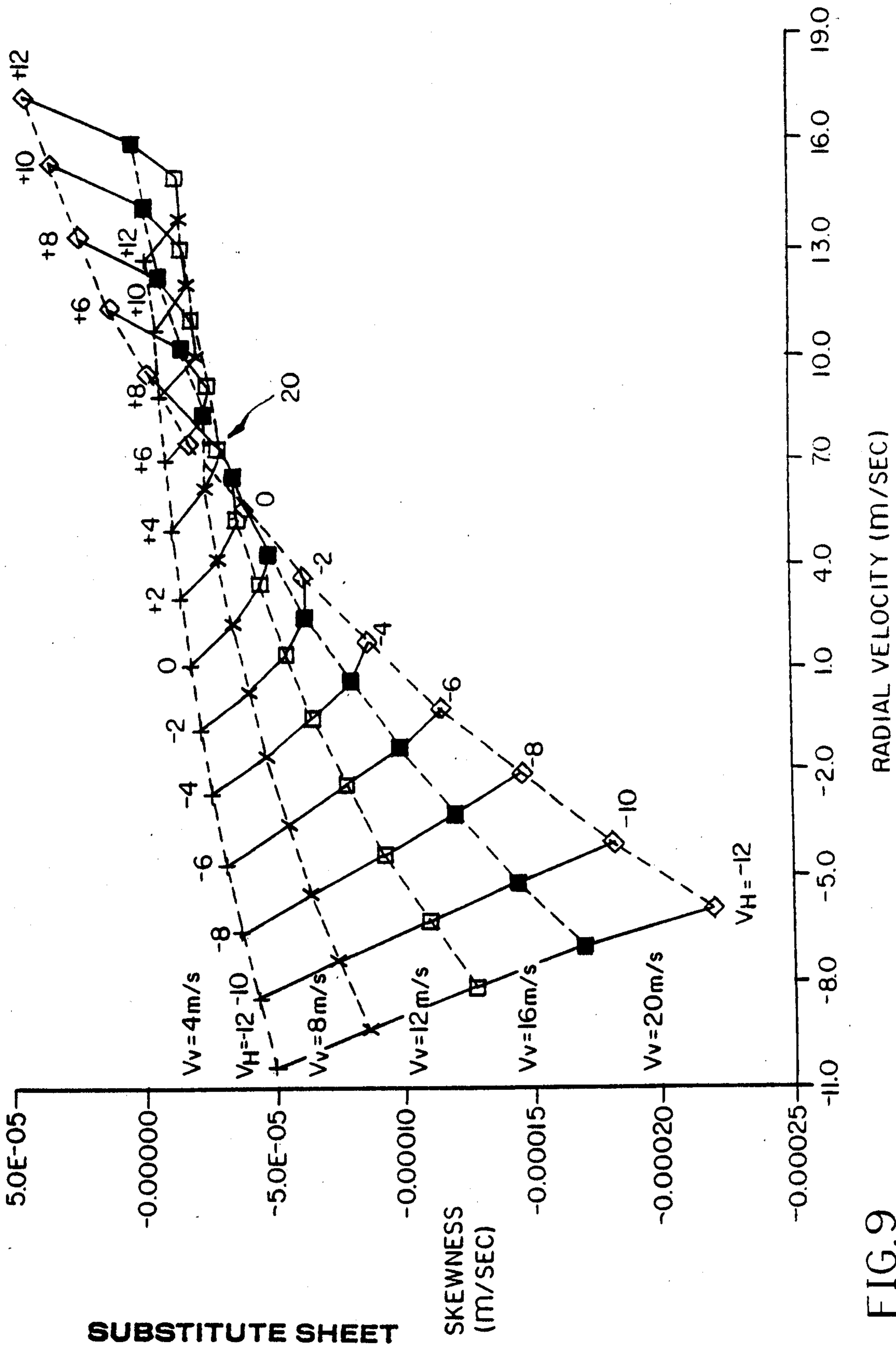
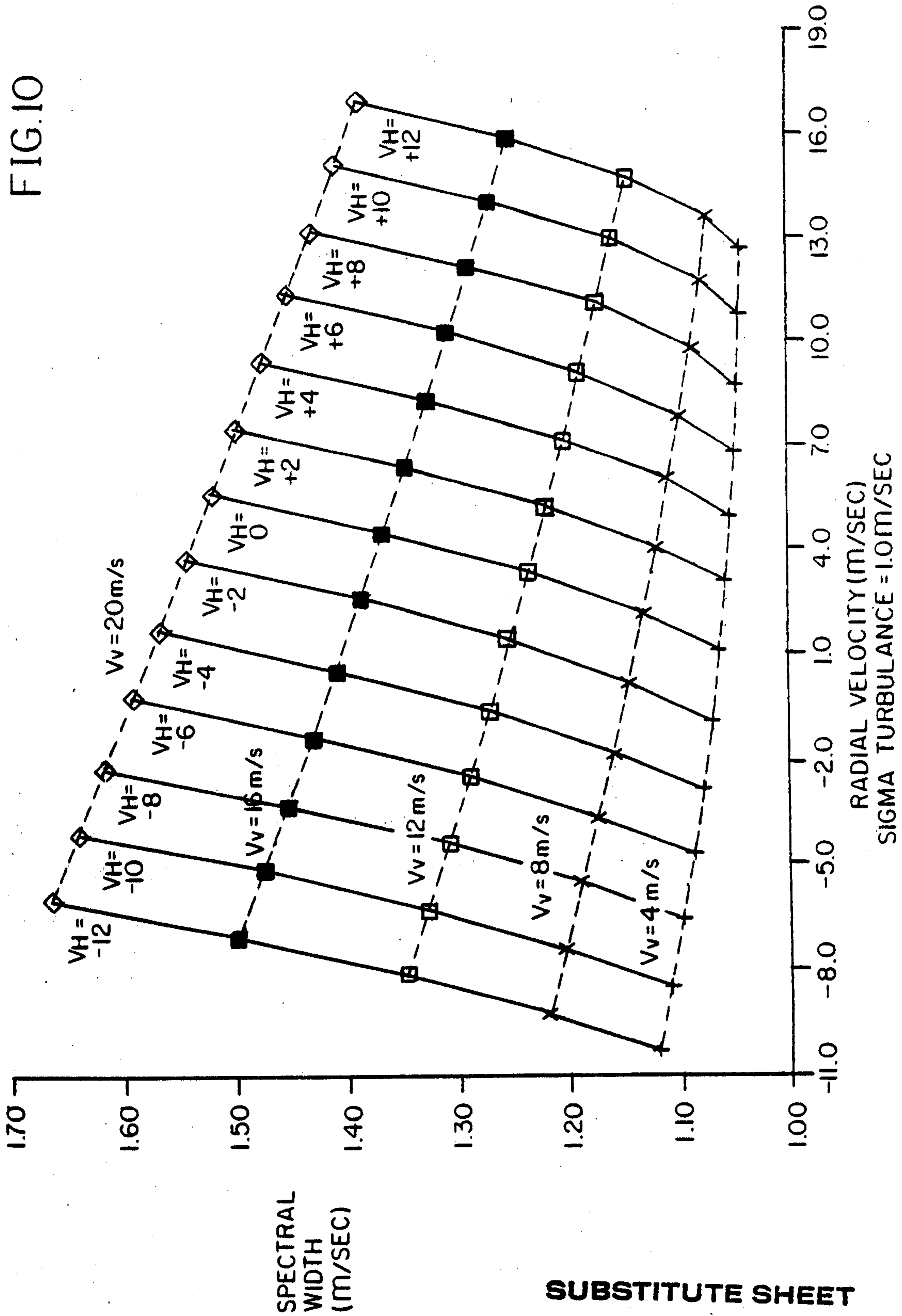


FIG.9

FIG.10



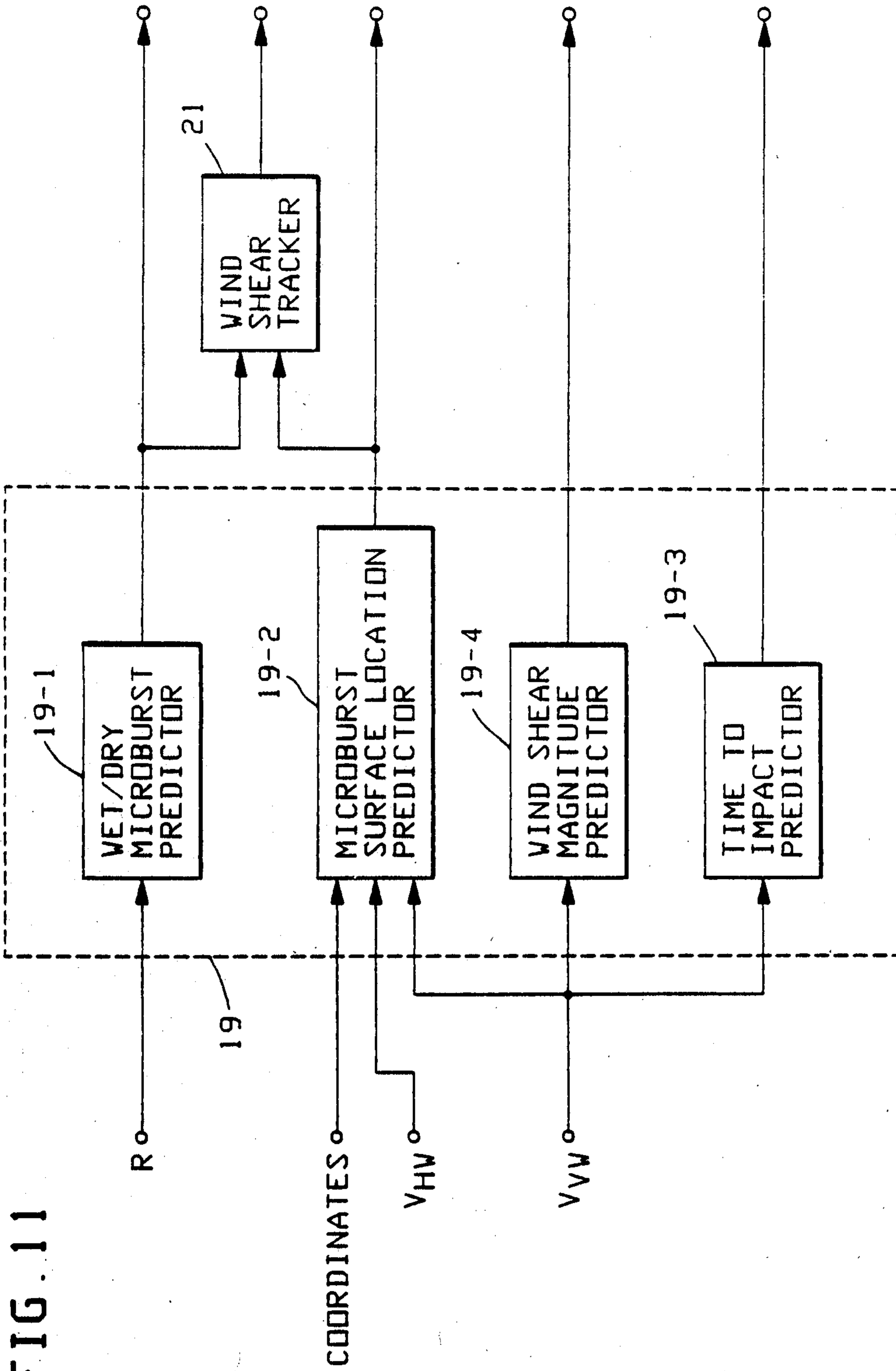


FIG. 11